Plasmonic Sensing of Biological Analytes Through Nanoholes

Grace M. Hwang, Lin Pang, Elaine H. Mullen, and Yeshaiahu Fainman, *Fellow, IEEE*

***Abstract*—A transmission-based surface plasmon resonance (SPR) sensor for label-free detection of protein–carbohydrate and protein–protein binding proximate to a perforated gold surface is demonstrated. An SPR instrument makes real-time measurements of the resonant wavelength and/or the resonant angle of incidence of transmitted light; both are influenced by the presence of proteins at the gold surface-liquid interface. Ethylene glycol solutions with known refractive indexes were used to calibrate the instrument. A paired polarization-sensitive detector achieved an overall detection resolution of $\sim 6.6 \times 10^{-5}$ refractive index units (RIU). Proof of principle experiments was performed with concanavalin A (Con A) binding to gold-adsorbed ovomucoid and anti-bovine serum albumin (BSA) binding to gold-adsorbed BSA.**

***Index Terms*—Bioplasmonics, biosensors, gold nanohole array, surface plasmon polariton (SPP), surface plasmon resonance (SPR).**

I. Introduction

THE deployment of biosensing systems that can rapidly detect and identify airborne and waterborne pathogens *in situ* with acceptable false alarm rates presents enormous challenges. For example, pathogens have been shown to spread exponentially via commercial airline traffic [1]. Numerous rapid biosensor technologies (reviewed in [2] and [3]) are being developed, but currently available systems fail to meet some or all of the performance criteria needed for large-scale deployment. These criteria include low false alarm probabilities ($P_{FA} \lesssim 10^{-4}$), highly sensitive detection for a wide range of bioagents (probability of detection $P_D > 0.9$), rapid response time (on the order of minutes or less), limited use of liquid consumable reagents, energy efficiency, and compact packaging. Here, we present a sensitive biosensor that is suited for highly parallel multi-analyte sensing in an energy efficient and compact footprint.

Manuscript received February 22, 2008; revised July 01, 2008; accepted August 12, 2008. Current version published November 19, 2008. This work was supported in part by The MITRE Corporation and in part by the Defense Advanced Research Projects Agency Center for Opto-Fluidic Integration. The associate editor coordinating the review of this paper and approving it for publication was Prof. Ralph Etienne-Cummings.

G. M. Hwang is with The MITRE Corporation, Bedford, MA 01730 USA (e-mail: gmhwang@mitre.org).

L. Pang and Y. Fainman are with the Department of Electrical and Computer Engineering, University of California at San Diego, La Jolla, CA 92093-0407 USA (e-mail: lpang@ece.ucsd.edu; fainman@ece.ucsd.edu).

E. H. Mullen is with The MITRE Corporation, McLean, VA 22102-7539 USA (e-mail: emullen@mitre.org).

Color versions of one or more of the figures in this paper are available online at http://ieeexplore.ieee.org.

Digital Object Identifier 10.1109/JSEN.2008.2007663

Surface plasmons (SPs) can be described as electron density waves formed at the interface of a metal and a dielectric. A surface plasmon polariton (SPP) is an oscillation in which the electron density wave from the metal is coupled with the photon from the excitation source [4]. Due to the large surface energy confinement of SPPs, they are extremely sensitive to perturbations in the index of refraction at the metal-dielectric interface. The most common commercially available surface plasmon resonance (SPR) method uses the prism-based Kretschmann–Raether geometry [5]. Recently, SPR techniques are experiencing a reemergence, largely due to advances in nanofabrication that have made it possible to excite surface plasmons using metallic subwavelength structures instead of prism coupling (reviewed in [6]–[11]). Enhanced transmission through metallic subwavelength structures already shows great promise for high throughput applications [12]–[17]. More importantly, many features of an SPR biosensor meet the requirements for compact, portable packaging and low power necessary for field deployment [18]–[20]. SPR systems do not require extrinsic fluorophore tags; they require only small quantities of consumables in typical assays, demonstrate near real-time detector responses, and can regenerate the sensing surface with a low pH wash. To date, prism-based SPR systems have been shown to detect proteins, bacteria, toxins, allergens, HIV, the West Nile Virus, and the SARS-associated corona virus [21]. Despite these benefits, conventional SPR designs are not as sensitive as fluorescence sensors that employ extrinsic labels.

In this paper, we discuss the use of an integrated microfluidic chip SPR biosensor configured in a transmission setup. The system consists of a nanohole array etched into a thin gold film [17], [22], [23] that is coated with carbohydrate receptor molecules to capture specific pathogens. The system was calibrated with a series of ethylene glycol solutions at controlled refractive indexes. A paired polarization-sensitive detector achieved an overall detection resolution of $\sim 6.6 \times 10^{-5}$ refractive index units (RIU). Motivated by recent findings which implicated the role of carbohydrate receptors in differentiating human from nonhuman influenza viruses [24], [25], we measured real-time interaction between an infectious agent simulant, conconavalin A (Con A) carbohydrate-binding lectin, and mannose carbohydrate receptors on the glycoprotein ovomucoid. In addition, real-time, label-free, protein–protein binding measurements were obtained using bovine serum albumin (BSA) and anti-BSA. Rough estimates of detection limits for Con A and BSA from the nanohole SPR sensor are discussed. We conclude with recommendations for carbohydrate receptor integration and our path forward on a design for

high throughput applications and methods to enhance system resolution and sensitivity.

II. Materials and Methodology

A. Materials

The SPP sample holder, consisting of a gold nanohole array on a glass slide and microfluidic channel ($10 \times 2 \times 0.1$ mm^3) molded in polydimethylsiloxane (PDMS), was prepared following standard holographic lithography patterning, described in our previous work [17], [22].

Mouse monoclonal antibody (MAb, B2901, ~140 kilo-Dalton [kD]), Albumin bovine fraction V power (BSA, A9647, ~66 kD), and the Protein A Antibody Purification Kit (PURE1A-1 Kt) were purchased from Sigma-Aldrich (Saint Louis, MO). MAb was purified with PURE1A-1 Kt; MAb recovery concentration was determined via UV absorption at 280 nm.

Ovomucoid from chicken egg white (Trypsin Inhibitor T9253, MW ~28 kD) was purchased from Sigma-Aldrich. Concanavalin A (Con A) (FL-1001, MW ~26.8 kD) was purchased from Vector Laboratories (Burlingame, CA).

All solutions were sterilized through a 0.2 μm-pore syringe filter (Fisherbrand, nylon).

B. Experimental Setup and Procedure

We previously explored resonant SPP transmission through a 2-D nanohole array in an angular setup [17]. In this prior work, using index-calibrated solutions to create a controlled refractive index in the overlayer at the gold-fluid interface, we reported that the resolving power and interrogation range were more sensitive in an angular than in a wavelength configuration. However, in terms of future system deployment, we prefer to build a setup that uses as few moving parts as possible. Thus, our experiments were conducted in a wavelength-interrogation configuration where the angle of incidence remained fixed after initial calibration. The period of the nanohole array was designed to match the illumination wavelength range. Nanoholes are approximately 300 nm in diameter and spaced 1.5 μm apart. Gold film thickness ranges between 150 and 200 nm. The propagation of coupled SPP modes on the grating coupler is described as

$$k_{\mathrm{SPP}} = \frac{\omega}{c} n_s \sin\theta \pm iG_x \pm jG_y \qquad (1)$$

where ω is the angular frequency, c is the speed of light in a vacuum, $\mathrm{n_s}$ is the refractive index of the dielectric overlayer, θ is the angle of incidence, and i and j are integer values. G_{x} and G_{y} are the reciprocal vectors for a square lattice with $|G_{\mathrm{x}}| = |G_{\mathrm{y}}| = 2\pi/a_o$, with a_o being the period [7], [26].

To measure the intensity of the SPP modes at the overlayer, we used a collimated tunable laser beam (<0.5 mm diameter) with 1-pm wavelength resolution (1520–1570 nm, 6.9 dBm, scan rate 100 nm/s, 5-trace averaging) to illuminate a sample area of 200×200 μm^2 on the gold nanohole array. As shown in Fig. 1, the sample holder was placed between an orthogonally crossed polarizer–analyzer pair in such a way that the surface wave was excited by a projection of the incident electric field polarization. The reradiated resonant field was then projected

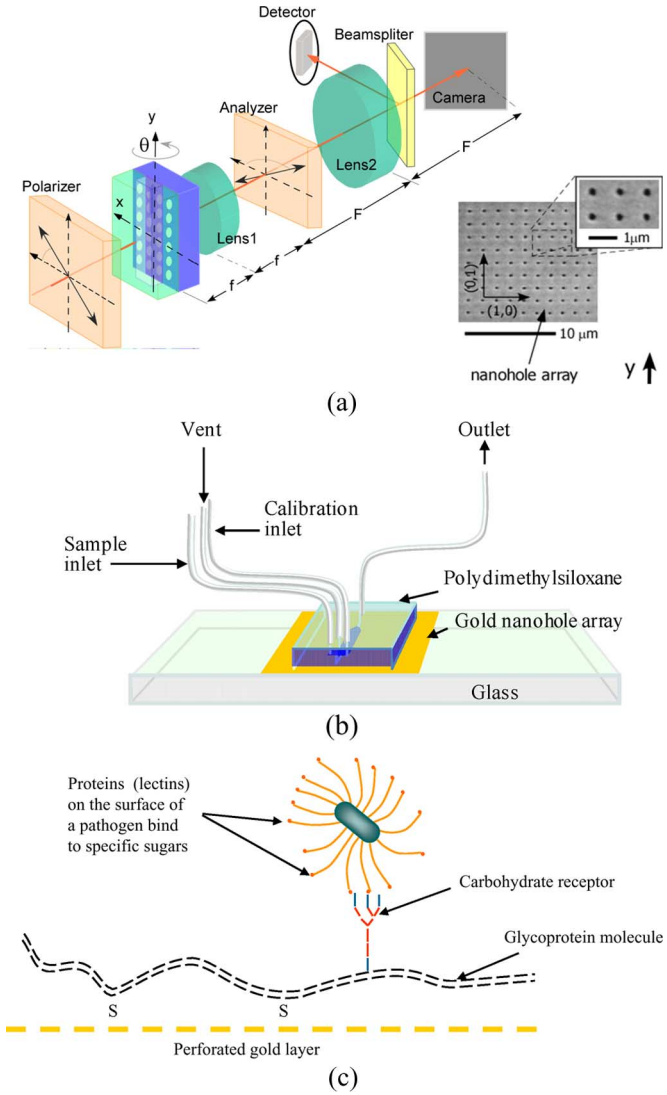

Fig. 1. (a) Schematic of the 2-D nanohole-array SPP transmission setup. Inset: scanning electron micrograph of a section of the gold nanohole array. (b) SPP sample holder. (c) Pathogen capture via carbohydrate receptor and protein binding.

onto the analyzer and the greater part of the nonresonant photon transmission was rejected. The transmitted light was simultaneously used to image the sample holder onto an InGaAs camera for alignment and to measure light transmission using a photodiode. Any change of the in-plane wave vector was achieved by rotating the sample in the $x - z$ plane (angle θ in Fig. 1) via a mechanized rotation stage with a 0.001° angle resolution.

The SPR transmission mechanism involves coupling to an SPP mode, evanescent transmission through the below-cutoff waveguide hole, and scattering of radiation again from the nanohole array to produce propagating free-space modes. Normalized transmittance spectra from wavelength interrogation are shown in Fig. 2(a) in the vicinity of the (1,0) type SPP mode from the overlayer solution. Transmission spectra were obtained at an incidence angle 18° from the normal.

Prior to each experiment, the sample holder was flushed with 5 ml of sterile, deionized (DI) water *in situ*. Then, ~3 ml of receptor molecules concentrated at 1 mg/ml were flowed into the

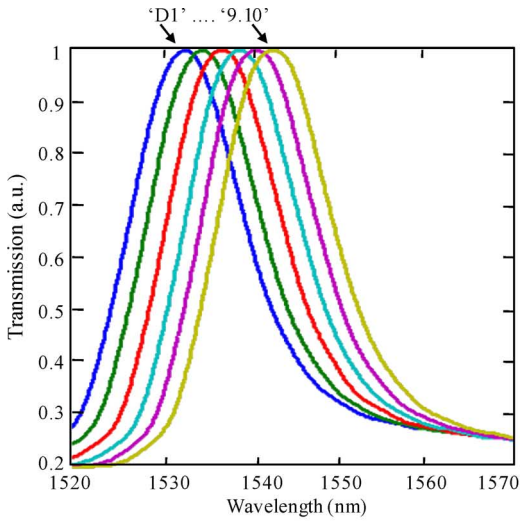

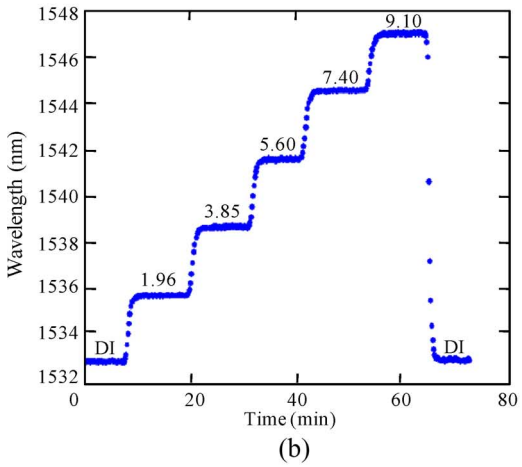

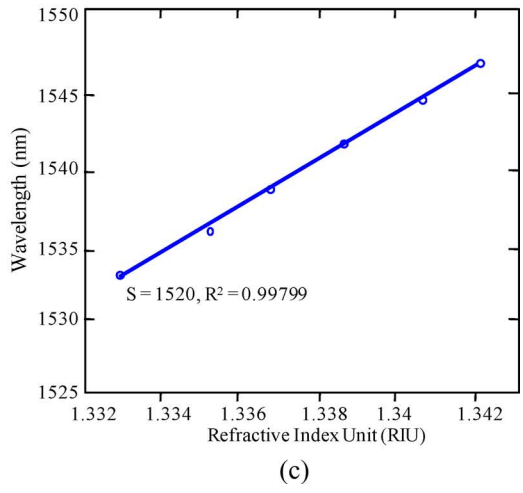

Fig. 2. (a) Normalized transmission spectra corresponding to ethylene glycol solution series (%): 0, 1.96, 3.85, 5.60, 7.40, 9.10. Data were obtained at an incidence angle 18° from the normal. (b) Representation of resonant wavelength versus time; EG concentration in percentages are shown. (c) Representation of resonant wavelength versus refraction index units (RIUs). The resonant wavelengths and RIUs are linearly related ($R^2 = 0.99$, Pearson's). Open circles represent data based on five-shot averaging. The line represents a linear fit to experimental data. Sensitivity $(S) = 1520$ nm/RIU. Total shift $= 13.9$ nm.

SPP sample holder, enabling the receptor molecules to adhere to the surface of the gold film via thiol-bond formation. Adsorption strength of thiol groups in Cysteine residues on gold surface depends on the deposition time as described in Section III. Excess receptor molecules were washed away with sterile DI water for 5 min. A microfluidic channel was used to transport analytes to the overlayer at a flow rate of ~ 100 μl/min.

C. Receptor Molecule Selection

In order to perform biological experiments using carbohydrate receptors we had to identify a suitable analyte-receptor pair. We utilized SugarBindDB, a web-enabled, searchable database that catalogs all known published data on carbohydrates expressed by host cells to which pathogenic bacteria, viruses, and biotoxins bind [27]. We targeted *Escherichia coli* K12 as a surrogate. We started by employing SugarBindDB to identify which complex carbohydrate would interact with *E. Coli's* Type 1 fimbriael adhesins. From the SugarBindDB search results, we recognized that the nonreducing terminal mannose should be sufficient for binding the fimbriae of *E. coli* K12. We then employed GlycoSuiteDB [28], a database that catalogs all known sugar sequences on glycoproteins by tissue type, to identify which glycoproteins naturally bear the carbohydrates we required, i.e., terminal mannose. Based on our findings in GlycoSuiteDB, the egg white protein ovomucoid was shown to have glycans with terminal mannose receptors. We recognized that the commercially available plant lectin Con A binds to both terminal mannose and to the trimanylsyl core common to all N-linked glycans; so it would suffice as a model surrogate for *E. Coli*. Therefore, we chose to use ovomucoid and Con A as our model receptor molecule and analyte pair to simulate pathogen capture.

III. Results

A series of ethylene glycol (EG) solutions ranging from 0% to 9% by volume was introduced into the microfluidic channel. Fig. 2(a) depicts normalized transmission spectra of the EG solution series. Fig. 2(b) shows the resonant wavelength as a function of time. At $t = 0$, the DI water was devoid of EG. The EG solutions were added to the channel in increasing concentrations of about 2% until a maximum of 9% EG was reached, as depicted by each jump along the time axis. Following the 9% EG test, DI water was introduced into the channel returning the SPP resonant wavelength to 1533 nm. (Accurate concentrations of the solution were 1.96%, 3.85%, 5.60%, 7.40%, and 9.10%.) The wavelength-time trace exhibited stability at each EG concentration and the increase in SPP resonant wavelength was proportional to the increase in EG concentration. Fig. 2(c) shows the resonant wavelength as a function of the refractive index of the fluid at the overlayer. The resonant wavelength and RIUs are linearly related ($R^2 = 0.99$, Pearson's). Open circles represent data based on five-shot averaging. The line represents a least squares linear regression on the experimental data, the slope of which approximates the sensitivity (S_λ) for the (1,0) type SPP mode, $S_\lambda = 1520$ nm/RIU. If we assume a system repeatability of 0.1 nm, then S_λ corresponds to a resolution of 6.6×10^{-5} RIU [0.1 nm/(1520 nm/RIU)].

We monitored the response of Con A to ovomucoid in the SPP setup. Prepared solutions consisted of: 1) 0.01 M phosphate-buffered saline (PBS) prepared by dissolving PBS powder in

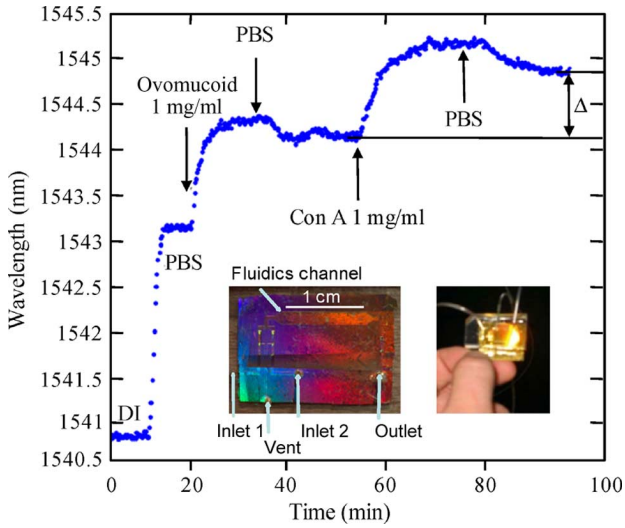

Fig. 3. Demonstration of protein–carbohydrate binding on a gold nanohole array observed by monitoring the resonant wavelength of a SPP mode at the fluid-metal overlayer in a transmission setup. Insets are photographs of an SPP sample holder with (right) and without (left) tubing.

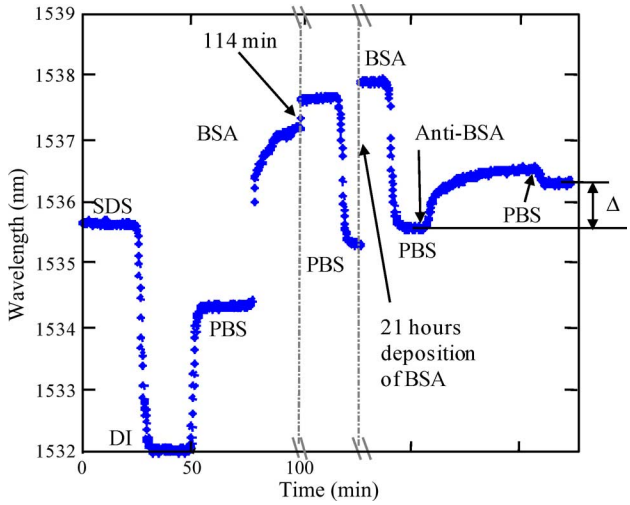

Fig. 4. Demonstration of protein–protein binding on a gold nanohole array observed by monitoring the resonant wavelength of a SPP mode at the fluid-metal overlayer in a transmission setup.

water with pH value of 7.4 at 25 °C; 2) 1 mg/ml Con A in PBS; and 3) an aqueous solution of ovomucoid (1 mg/ml) heated for 10 min at 95 °C, stirred for 30 min, passed through a 0.2-μ m-pore syringe filter (Fisherbrand, nylon) and allowed to cool on ice.

The integrated microfluidic SPR sensor device was pretreated with DI water for 8 min. The PBS solution was then introduced and run for 10 min, shifting the resonant wavelength to 1543.2 nm (Fig. 3); this defined the base line of the sensor for this experiment. Solution with 1 mg/ml of ovomucoid was then introduced into the channel. After the ovomucoid solution was run for 11 min, PBS was added to the channel for flushing away excess unbound ovomucoid, leading to a resonant wavelength shift to 1544.2 nm. After flowing PBS for 20 min, the purified Con A solution was introduced into the channel to allow for specific binding to the ovomucoid attached to the gold surface. After 25 min, PBS was introduced to wash out the unbound Con A, although disassociation of weakly bound ovomucoid from gold surface could also have occurred. The resulting resonant wavelength was 1544.9 nm, which corresponds to a binding shift Δ of 0.7 nm.

The laser we employed did not have a wavelength scan repeatability comparable to state-of-the-art components. In order to obtain a rough estimate of the detection limit of our sensor system, we considered the combination of the repeatability of the light source and the background of the detector (χ), which was the estimated standard deviation of the actual wavelength variance at scan mode. Using established extrapolation methods [29], [30], we defined a scaling factor M as the ratio Δ/χ, such that $\chi = 0.1$ nm corresponds to an M of 7. We then estimated the detection limit as the ratio of the actual analyte concentration to the scaling factor M. Thus, the system presented here has an estimated detection limit of $\sim$ 143 μg/ml $(\sim 5.3\ \mu\text{M})$ for Con A, which would be greatly improved by an upgraded laser scan and detection system. It is worth mentioning that resonant shifts in the above and following tests were obtained by only locating the maximum from each raw SPP transmission spectrum. Further data analysis and processing will be employed to increase the accuracy of identifying SPP resonant peaks [31]. Different data fit functions, including Lorentian, Fano-type, and polynomial line shapes for SPP resonant are being investigated.

Though the main focus of this paper is on the use of carbohydrate receptors to capture model pathogens, in connection with the larger SPP biosensing field, we also investigated protein–protein (pathogen simulant-antibody) binding. We monitored the response of monoclonal anti-bovine serum albumin (mAb) to BSA in the SPP setup. Prepared solutions consisted of: 1) 2 wt % of sodium dodecyl sulfate (SDS) in water; 2) 0.01 M PBS prepared by dissolving PBS powder in water with pH value of 7.4 at 25 °C; 3) 2 mg/ml BSA in PBS prepared by dissolving BSA in water, adding 2-mercaptoethanol (MER) into 2 mg/ml BSA to make a 1% MER BSA PBS solution; and 4) purifying monoclonal anti-BSA with Protein A Antibody Purification Kit and dissolving it into PBS to attain 0.293 mg/ml, verified by ultraviolet absorbance (not shown), diluted to make about 26.6 μg/ml anti-BSA PBS solution. Using a molecular weight of 140 kD for anti-BSA, the estimated anti-BSA concentration was $\sim$190 nM.

The integrated microfluidic SPR sensor device was first cleaned by running 2% SDS solution for about 30 min through the surface of the gold nanohole array (Fig. 4) producing a resonant wavelength of 1535.8 nm. The SDS solution was then replaced by a water rinse for 20 min. The PBS solution was then introduced and run for 22 min, shifting the resonant wavelength to 1534.4 nm; this defined the base line of the sensor for this experiment. BSA solution with 1% MER was then introduced into the channel. After the BSA solution was run for 26 min data acquisition was stopped, but the BSA solution was kept flowing for an additional 114 min. After data monitoring was turned back on, PBS solution was introduced into the channel for 14 min to wash out the excess, unattached BSA. A resonance measurement showed that attachment of the BSA to the gold surface produced a resonant wavelength

shift to 1535.4 nm. BSA solution was then introduced into the channel again with the flow rate reduced to a very slow speed to allow more BSA to adhere to the gold surface. After 21 h, the pressure difference between inlet and outlet was reset to produce an original flow rate ($\sim$ 75 μl/min) and resonance data acquisition was restored. Ten minutes later, PBS was added to the channel for flushing, leading to a resonant wavelength shift to 1535.6 nm. After flowing PBS for 15 min, the purified monoclonal anti-BSA solution was introduced into the channel to allow for specific binding to the BSA attached to the gold surface. After 60 min, PBS was introduced to wash out the unbound anti-BSA, although disassociation of weakly bound BSA from gold surface could also have occurred. The resulting resonant wavelength was 1536.3 nm, which corresponds to a binding shift Δ of 0.7 nm. It is a coincidence that the final binding shift is the same in Figs. 3 and 4, likely due to a combination of differences in the molecular weight of the analytes and the deposition density of the receptor molecules.

IV. Discussion

It is well known that the strength of the binding interaction process depends on many factors. These include the quantity of bound receptors and the strength of their attachment to the gold surface. In order to achieve a strong attachment of the receptors, in most cases a self-assembled monolayer (SAM) is applied to the gold surface as the linker layer, so that one SAM end-group binds strongly to the gold surface while the other SAM end-group will effectively connect the receptors. Instead of using a SAM, we added 2-mercaptoethanol into the BSA solution to prevent the oxidation of free sulphydryl residues in the BSA. Two hours of flowing BSA MER solution led to a resonant wavelength shift of 1.0 nm for attachment to the gold surface, with an additional 20 h of flowing producing an additional 0.3-nm wavelength shift. Therefore, the total BSA attachment produced a 1.3-nm wavelength shift compared to the PBS base line resonance. By comparison, 23 h flowing of BSA solution without 2-mercaptoethanol produced only 0.6-nm resonance shift from BSA attachment (not shown). The 2-mercaptoethanol indeed improves the attachment of BSA to a gold surface.

To estimate an ideal detection limit for our transmission-based SPR nanohole sensor, we need to consider the absolute best χ one could achieve. A light source with χ less than 1 pm [32] would allow us to estimate the detection limit with scaling factors as large as 700. Thus, the system presented here has the potential to detect Con A down to 1.43 μg/ml (or $\sim$53 nM) and to detect anti-BSA down to 38 ng/ml (or $\sim$271 pM). This analysis suggests that an extremely sensitive detection limit is achievable in a transmission setup.

We realize that a simultaneous blank would be advantageous. Currently, we are designing a PDMS fluidics chip with built-in temperature controls and a reference channel to perform simultaneous blanks to reduce the probability of false alarms.

We employed carbohydrate receptor molecules following recent work which has demonstrated their ability to distinguish human influenza from avian influenza. We show the utility of glycobiology databases (e.g., SugarBindDB and GlycoSuiteDB) for guiding receptor molecule selection to capture pathogens of interest. Shinya *et al.* demonstrated that human-derived influenza viruses that bind to epithelial cells located in the upper respiratory tract preferred the carbohydrate receptor molecule sialic acid α2–6 galactose, whereas avian influenza viruses (e.g., H5N1) predominantly bind to the carbohydrate receptor molecule sialic acid α2–3 galactose present on alveolar cells in the lower human respiratory tract [25]. More recently, Chandrasekaran *et al.* reported that the sialic acid α2–6 galactose trisaccharide receptor molecules that bind to human influenza viruses are umbrella-shaped, whereas the sialic acid α2–3 galactose trisaccharide receptor molecules that bind to avian influenza viruses are cone-shaped. This provides a topological explanation for why the complementary protein lectin of H5N1 prefers sialic acid α2–3 galactose [24]. Collectively, these findings suggest the importance of carbohydrate receptor binding specificities for differentiating human from nonhuman influenza viruses. In the future, we plan to use *E. coli* K12 and a nonvirulent strain of influenza for testing this approach.

V. Conclusion

We have implemented a label-free method to utilize glycoproteins as carbohydrate receptor molecules on a gold nanohole array to capture pathogen simulants in a transmission-based nanohole array SPR setup. We devised a method that utilizes glycomics databases to guide the design of receptor molecules for use inside a biosensor. We showed, through estimates, that our SPR sensor can be improved to exhibit picomolar detection limits. In the future, we will explore methods to improve wavelength illumination repeatability, experiment with different illumination wavelength bands, model nanohole performance as a function of diameter and lattice spacing, and fabricate different types of nanostructures to enhance overall system resolution and sensitivity. We will also increase the total number of sensing elements in the PDMS mold in order to perform highly parallel multi-element SPR detection.

References

[1] A. Mangili and M. A. Gendreau, "Transmission of infectious diseases during commercial air travel," *Lancet*, vol. 365, pp. 989–996, 2005.
[2] J. J. Gooding, "Biosensor technology for detecting biological warfare agents: Recent progress and future trends," *Anal. chim. Acta*, vol. 559, pp. 137–151, 2006.
[3] N. O. Fischer, T. M. Tarasow, and J. B. H. Tok, "Heightened sense for sensing: Recent advances in pathogen immunoassay sensing platforms," *Analyst*, vol. 132, pp. 187–191, 2007.
[4] H. Raether, *Surface Plasmons on Smooth and Rough Surfaces and on Gratings*. Berlin: Springer, 1988, vol. 111, Springer Tracts in Modern Physics.
[5] Biacore, Flexchip Product Information 2006, Product description.
[6] R. L. Rich and D. G. Myszka, "Survey of the year 2005 commercial optical biosensor literature," *J. Molecular Recognition*, vol. 19, pp. 478–534, 2006.
[7] C. Genet and T. W. Ebbesen, "Light in tiny holes," *Nature*, vol. 445, pp. 39–46, 2007.
[8] J. Homola, "Present and future of surface plasmon resonance biosensors," *Anal. Bioanal. Chem.*, vol. 377, pp. 528–539, 2003.
[9] R. Ince and R. Narayanaswamy, "Analysis of the performance of interferometry, surface plasmon resonance and luminescence as biosensors and chemosensors," *Anal. Chim. Acta.*, vol. 569, pp. 1–20, 2006.
[10] K. Phillips and Q. Cheng, "Recent advances in surface plasmon resonance based techniques for bioanalysis," *Anal. Bioanal. Chem.*, vol. 387, pp. 1831–1840, 2007.

[11] N. Ramachandran, D. N. Larson, P. R. H. Stark, E. Hainsworth, and J. LaBaer, "Emerging tools for real-time label-free detection of interactions on functional protein microarrays," *Febs J.*, vol. 272, pp. 5412–5425, 2005.
[12] A. D. Leebeeck, L. K. Swaroop Kumar, V. de Lange, D. Sinton, R. Gordon, and A. G. Brolo, "On-chip surface-based detection with nanohole arrays," *Anal. Chem.*, vol. 79, pp. 4094–4100, 2007.
[13] G. Steiner, "Surface plasmon resonance imaging," *Anal. Bioanal. Chem.*, vol. 379, pp. 328–331, 2004.
[14] A. G. Brolo, R. Gordon, B. Leathem, and K. L. Kavanagh, "Surface plasmon sensor based on the enhanced light transmission through arrays of nanoholes in gold films," *Langmuir*, vol. 20, pp. 4813–4815, 2004.
[15] T. W. Ebbesen, H. J. Lezec, H. F. Ghaemi, T. Thio, and P. A. Wolff, "Extraordinary optical transmission through sub-wavelength hole arrays," *Nature*, vol. 391, pp. 667–669, 1998.
[16] M. E. Stewart, N. H. Mack, V. Malyarchuk, J. A. N. T. Soares, T.-W. Lee, S. K. Gray, R. G. Nuzzo, and J. A. Rogers, "Quantitative multispectral biosensing and 1D imaging using quasi-3D plasmonic crystals," *Proc. Nat. Acad. Sciences*, vol. 103, pp. 17143–17148, 2006.
[17] K. A. Tetz, L. Pang, and Y. Fainman, "High-resolution surface plasmon resonance sensor based on linewidth-optimized nanohole array transmittance," *Opt. Lett.*, vol. 31, pp. 1528–1530, 2006.
[18] T. M. Chinowsky, M. S. Grow, K. S. Johnston, K. Nelson, T. Edwards, E. Fu, and P. Yager, "Compact, high performance surface plasmon resonance imaging system," *Biosens. Bioelectron.*, vol. 22, pp. 2208–2215, 2007.
[19] T. M. Chinowsky, S. D. Soelberg, P. Baker, N. R. Swanson, P. Kauffman, A. Mactutis, M. S. Grow, R. Atmar, S. S. Yee, and C. E. Furlong, "Portable 24-analyte surface plasmon resonance instruments for rapid, versatile biodetection," *Biosens. Bioelectron.*, vol. 22, pp. 2268–2275, 2007.
[20] A. N. Naimushin, C. B. Spinelli, S. D. Soelberg, T. Mann, R. C. Stevens, T. Chinowsky, P. Kauffman, S. Yee, and C. E. Furlong, "Airborne analyte detection with an aircraft-adapted surface plasmon resonance sensor system," *Sensor. Actuat B-Chem.*, vol. 104, pp. 237–248, 2005.
[21] G. P. Anderson, E. C. Merrick, S. A. Trammell, T. M. Chinowsky, and D. K. Shenoy, "Simplified avidin-biotin mediated antibody attachment for a surface plasmon resonance biosensor," *Sens. Lett.*, vol. 3, pp. 151–156, 2005.
[22] L. Pang, K. A. Tetz, and Y. Fainman, "Observation of the splitting of degenerate surface plasmon polariton modes in a two-dimensional metallic nanohole array," *Appl. Phys. Lett.*, vol. 90, p. 111103, 2007.
[23] K. A. Tetz, R. Rokitski, M. Nezhad, and Y. Fainman, "Excitation and direct imaging of surface plasmon polariton modes in a two-dimensional grating," *Appl. Phys. Lett.*, vol. 86, p. 111110, 2005.
[24] A. Chandrasekaran, A. Srinivasan, R. Raman, K. Viswanathan, S. Raguram, T. M. Tumpey, V. Sasisekharan, and R. Sasisekharan, "Glycan topology determines human adaptation of avian H5N1 virus hemagglutinin," *Nat. Biotech.*, vol. 26, pp. 107–113, 2008.
[25] K. Shinya, M. Ebina, S. Yamada, M. Ono, N. Kasai, and Y. Kawaoka, "Avian flu: Influenza virus receptors in the human airway," *Nature*, vol. 440, pp. 435–436, 2006.
[26] H. F. Ghaemi, T. Thio, D. E. Grupp, T. W. Ebbesen, and H. J. Lezec, "Surface plasmons enhance optical transmission through subwavelength holes," *Phys. Rev. B*, vol. 58, p. 6779, 1998.
[27] "Glycan database (http://sugarbinddb.mitre.org)," *Glycobiology*, vol. 15, pp. 9G–14G, 2005.
[28] C. A. Cooper, H. J. Joshi, M. J. Harrison, M. R. Wilkins, and N. H. Packer, "GlycoSuiteDB: A curated relational database of glycoprotein glycan structures and their biological sources. 2003 update," *Nucl. Acids Res.*, vol. 31, pp. 511–513, 2003.
[29] L. Pang, G. M. Hwang, B. Slutsky, and Y. Fainman, "Spectral sensitivity of two-dimensional nanohole array surface plasmon polariton resonance sensor," *Appl. Phys. Lett.*, vol. 91, p. 123112, 2007.
[30] W. Yuan, H. P. Ho, C. L. Wong, S. K. Kong, and C. L. Lin, "Surface plasmon resonance biosensor incorporated in a Michelson interferometer with enhanced sensitivity," *IEEE Sensors J.*, vol. 7, pp. 70–73, 2007.
[31] A. B. Dahlin, J. O. Tegenfeldt, and F. Hook, "Improving the instrumental resolution of sensors based on localized surface plasmon resonance," *Analytical Chemistry*, vol. 78, pp. 4416–4423, 2006.
[32] A. M. Armani, R. P. Kulkarni, S. E. Fraser, R. C. Flagan, and K. J. Vahala, "Label-free, single-molecule detection with optical microcavities," *Science*, vol. 317, pp. 783–787, 2007.

Grace M. Hwang received the B.S. degree in civil and environmental engineering from Northeastern University, Boston, MA, in 1996, the S.M. degree in civil engineering from the Massachusetts Institute of Technology, Cambridge, in 1998, and the M.S. and Ph.D. degrees in biophysics and structural biology from Brandeis University, Waltham, MA, in 2004 and 2005, respectively.

She worked at Raytheon Company between 1990 and 2000, where she developed a variety of optical systems for chemical analysis and biological detection. At Brandeis University, she developed a confocal microscopy system with single-molecule resolution for fluorescent correlation spectroscopy of proteins. In 2000, she joined The MITRE Corporation, Bedford, MA, a not-for-profit federally funded research and development center in the U.S. She is presently a Lead Biosensors Scientist. Her current research interests include biosensor development based on surface plasmon resonance and bioaerosol sensor design and integration.

Lin Pang received the B.S. and M.S. degrees in physics from Lanzhou University, Lanzhou, China, in 1987 and 1990, respectively, and the Ph.D. degree in optics from Sichuan University, Sichuan, China, in 1998, with a thesis on the fabrication of microstructures.

Since 2001, he has been a Project Scientist with the Ultrafast and Nanoscale Optics Group, University of California at San Diego, La Jolla. His current interests include the holographic lithography, photonic crystal, nanostructure fabrication, and biosensors based on surface plasmon resonance.

Elaine H. Mullen received her education in biology and biochemistry from Virginia Commonwealth University, Richmond, and The Johns Hopkins University, Baltimore, MD.

As a Research Scientist at The MITRE Corporation, McLean, VA, she studies bioactive properties of patented glycoprotein films. To support the development of glycoprotein biocapture films, she initiated an ongoing effort to list publications on carbohydrate receptors of human pathogens. Her current research includes a collaborative effort involving the Consortium for Functional Glycomics and the U.S. Department of Agriculture to precisely define carbohydrate affinities of pathogens responsible for food- and waterborne-illness.

Yeshaiahu Fainman (F'03) received the Ph.D. degree from Technion–Israel Institute of Technology, Haifa, Israel, in 1983.

He is a Cymer Professor of Advanced Optical Technologies and Professor of Electrical and Computer Engineering at the University of California at San Diego, La Jolla. His current research interests are in optical signal and information processing of ultrafast signals using both linear and nonlinear optical processes; nonlinear space-time processes using femtosecond laser pulses for optical communications, quantum cryptography, and communication; near field phenomena in optical nanostructures and nanophotonic devices; diffractive and nonlinear optics; and multidimensional quantitative imaging. He has contributed 200 manuscripts in refereed journals and over 350 conference presentations and conference proceedings.

Dr. Fainman is a Fellow of the Optical Society of America and Fellow of the Society of Photo-Optical Instrumentation Engineers. His honors and awards include the Miriam and Aharon Gutvirt Prize, Technion, Haifa, Israel (1982), Lady Davis Fellowship (2006), and Brown award (2006). He Chaired and co-Chaired various conferences including IEEE/LEOS sub-Committee on Optical Interconnects and Signal Processing, 2004–2008, and served as a General Chair for Inaugural OSA Topical Meeting on Nanophotonics for Information Systems, 2005. He also served on numerous conference program committees, organized symposia and workshops, and between 1993 and 2001 served as a Topical Editor of the *Journal of the Optical Society of America: A—Optical Signal Processing and Imaging Science*. He served as Associate Editor for *The European Physical Journals—Applied Physics*, in 2004–2006, and is currently serving as Editor for the *International Journal on Optical Memory and Neural Networks*, since 1998. He is an Editorial Board Member of *Nanotechnology Journal* and is serving on the Advisory Board for the journal *Metamaterials*.